Proceedings of the 4th WSEAS International Conference on Fluid Mechanics and Aerodynamics, Elounda, Greece, August 21-23, 2006 (pp136-141)

Implicit Stabilization Method for Numerical Modeling of Fluid Dynamics Problems

V. K. ARTEMYEV
Institute for Physics and Power Engineering, State Scientific Center of Russian Federation
Bondarenko Sq.1, Obninsk, Kaluga Region, 249033
RUSSIA
artemyev@ippe.ru

Abstract: - In this work, implicit numerical method for solving 2D and 3D-dimensional fluid mechanics, heat and mass transfer equations is presented. Discretization of governing equations is carried out on the base of monotonous balance neutral (MBN) difference schemes which allow to keep some important integral properties of differential operators. A difference equation for pressure is derived from the difference continuity and momentum equations. The discrete equations obtained are nonlinear so linearization is introduced and implicit stabilization iterative procedure is developed for yielding convergent solution. Explicit incomplete factorization method is employed for solving linearized momentum, heat and mass transfer difference equations and a variant of the method using Chebyshev acceleration is applied for solving pressure equation. Results of 2D two-phase flow and 3D natural convection numerical studies are presented.

Key-Words: - Fluid mechanics, heat and mass transfer equations, implicit numerical stabilization method, incomplete factorization method, two-phase flow, natural convection

1 Introduction

Implicit numerical technique [1-2] was successfully employed in analysing fluid mechanics, heat and mass transfer problems mainly for incompressible forced convection flows. At present method is developed for numerical prediction of natural and mixed convection problems, two-phase flows and others.

In general case, fluid dynamics processes are governed by a system of partial differential equations which involves continuity, momentum, heat and mass transfer equations, state equation etc. In a vector form continuity equation and equations of motion (Reynolds equations) may be written as follows:

$$\frac{\partial \rho}{\partial t} + div\,\rho\vec{\mathbf{U}} = 0, \vec{\mathbf{U}} = (u^1, u^2, u^3), \quad (1)$$

$$\rho\left(\frac{\partial \vec{\mathbf{U}}}{\partial t} + (\vec{\mathbf{U}}\nabla)\vec{\mathbf{U}}\right) = \rho\vec{\mathbf{F}} - \nabla p + 2\,div\,\mu\,\mathbf{Y} \\ -\frac{2}{3}\nabla(\mu\,div\,\vec{\mathbf{U}} + \rho K). \quad (2)$$

Momentum equations have been formulated accounting for the Bossiness hypothesis between stress tensor p^{ij} and velocity deformation tensor ε^{ij} components

$$p^{ij} = -pg^{ij} + 2\mu\varepsilon^{ij} - 2/3g^{ij}(\mu\,div\,\vec{\mathbf{U}} + \rho K), \quad (3)$$

where ρ is a density, $\mu = \mu_m + \mu_t$ – a coefficient of molecular and turbulence viscosity, g^{ij} are components of the Euclidean metric tensor, p is a pressure, K – a turbulent kinetic energy, $\vec{\mathbf{U}}$ – a velocity vector, **Y** – the tensor of velocity deformation, $\vec{\mathbf{F}}$ – a body force vector.

If heat transfer processes are under consideration than system (1)-(3) is added by an energy equation

$$\rho\left(\frac{\partial h}{\partial t} + \vec{\mathbf{U}}\nabla h\right) = \frac{dp}{dt} + q_v - div\,\vec{\mathbf{q}}, \quad (4)$$

where h is a enthalpy, q_v - a volumetric heat generation, $\vec{\mathbf{q}}$ – a heat flux.

2 Difference Approximations

Discretization of governing equations is carried out using monotonous balance neutral (MBN) difference schemes which allow to keep some important integral properties of differential operators. A derivation MBN difference scheme is based upon joint consideration of continuity equation and transfer equation.

For the sake of simplicity, consider the following system in a bounded domain Ω

$$\frac{\partial \rho}{\partial t} + \frac{\partial \rho u^i}{\partial x^i} = 0, \; i = \overline{1,n}, \quad (5)$$

$$\rho \frac{\partial \varphi}{\partial t} + \Lambda(\varphi) = f\,, \qquad (6)$$

where $\Lambda(\varphi) \equiv \rho u^i \frac{\partial \varphi}{\partial x^i} - \frac{\partial}{\partial x^i} \eta^{ii} \frac{\partial \varphi}{\partial x^i}$.

A substance φ may be a velocity component, an enthalpy, a concentration, etc. A monotonous schemes simulate important property of a fluid flow as a downstream transfer of some disturbance due to a convection motion. A balance (conservation) property is a discrete analogue of the Ostrogradski-Gauss theorem:

$$\frac{\partial}{\partial t} \int_{\Omega} \rho \varphi d\,\Omega = \int_{\Omega} f\, d\,\Omega - \int_{\Sigma} \rho \varphi u^i\, e_i\; d\Sigma + + \int_{\Sigma} \eta^{ii} \frac{\partial \varphi}{\partial x^i} e_i\, d\Sigma\,, \qquad (7)$$

where $\vec{\mathbf{e}}$ is the unit vector normal to the boundary Σ. Another property of the operator $\Lambda(\varphi)$ concerns null contribution of the terms describing connection transfer to the energy dissipation law. Neutral behaviour may be formulated in the form of the integral relationship,

$$\int_{\Omega} \frac{\rho \varphi^2}{2} d\Omega \Big|_0^{t_0} + \int_0^{t_0} dt \int_{\Sigma} \vec{\mathbf{U}}\, \vec{\mathbf{e}}\, \frac{\rho \varphi^2}{2} d\Sigma = \int_0^{t_0} dt \int_{\Omega} f\, \varphi d\;\Omega + \int_0^{t_0} dt \int_{\Sigma} \eta^{ii} \frac{\partial \varphi}{\partial x^i} \varphi\; d\Sigma - . - \int_0^{t_0} dt \int_{\Omega} \eta^{ii} \frac{\partial \varphi}{\partial x^i} \frac{\partial \varphi}{\partial x^i}\; d\,\Omega \qquad (8)$$

The account of the property (8) is especially important during long-time numerical simulation of fluid dynamics problems.

Grid points and grid spacings are defined in a regular region Π ($\Omega \in \Pi$) as:

$$x_b^i \le x_{1/2}^i < x_{3/2}^i < \ldots < x_{k_i}^i < \ldots < x_{N_i+1/2}^i \le x_e^i\,,\;;$$

$$k_i = \overline{1, N_i}\;\;, i = \overline{1,n}$$

$$x_{k_i}^i = 0.5(x_{k_i+1/2}^i + x_{k_i+1/2}^i)\,,\; k_i = \overline{1, N_i}\;,\; i = \overline{1,n}\,;$$

$$h_{k_i-1/2}^i = x_{k_i}^i - x_{k_i-1}^i\;,\; k_i = \overline{2, N_i}\,,\; i = \overline{1,n}\;\;;$$

$$h_{k_i-1/2}^i = 0.5 \cdot h_{k_i}^i\;\;\;,\; k_i = 1,\; i = \overline{1,n}\;\;;$$

$$h_{k_i-1/2}^i = 0.5 \cdot h_{k_i-1}^i\;,\; k_i = N_i + 1,\; i = \overline{1,n}\,;$$

$$h_{k_i}^i = x_{k_i+1/2}^i - x_{k_i-1/2}^i\;,\; k_i = \overline{1, N_i}\,,\; i = \overline{1,n}\;\;,$$

where $k = (k_1,...,k_n)$ is a multi–index m – a time step number, $\Delta\, t_{\,m}$ - a spacing of time discretization, In the following formulas the shortened notations of grid function are used:

$\varphi_{k_1,...k_i,...,k_n} \equiv \varphi_k$, $\varphi_{k_1,...k_i \pm 1,...,k_n} \equiv \varphi_{k+i}$,

$\varphi_{k_1,...k_i \pm 1/2,...,k_n} \equiv \varphi_{k \pm i/2}$,

$i(or\;\; j) = (0,...,1,...,0)$ is a multi- index, having unit in the i(or j)–position. The equation (9) is not directly included in the implicit iterative procedure but is the base for derivation of pressure difference equation.

Pressure, temperature, concentration are computed in the centres of elementary volume $V_e = \prod_{j=1}^{n} [\, x_{k_j-1/2}^j , x_{k_j+1/2}^j\,]$, components of velocity vector - in the centres of faces. Both the MBN–scheme and a displacement of coordinates of a grid functions enable to obtain physically realistic fields of computed values.

Difference continuity equation is written as

$$\xi_k^{\,m+1} \equiv \frac{\rho_k^{m+1} - \rho_k^{m}}{\Delta t_m} + + \sum_{j=1}^{n} \frac{(\rho\, u^j)_{k+j/2}^{m+1} - (\rho\, u^j)_{k-j/2}^{m+1}}{h_{k_j}^j} = 0\,, \qquad (9)$$

Transfer equation (6) is integrated over an elementary volume shifted in a i-direction (in comparison with V_e)

$$V_e^i \equiv \prod_{j=1}^{n} [\, x_{k_j + \delta^{ji}/2 - 1/2}^j , x_{k_j + \delta^{ji}/2 + 1/2}^j \;]\;\;,$$

$\delta^{i\,j}$ – Kronecher's symbol. MBN approximation of equation (6) has the following form:

$$\prod_{\beta=1}^{n} h_{k_\beta + \delta^{\beta i}/2}^{\beta}\; \rho_{k+i/2}^{m} \frac{\varphi_{k+i/2}^{\,m+1} - \varphi_{k+i/2}^{\,m}}{\Delta t_{\,m}} + + A(\varphi_{k+i/2}^{m+1}) = \prod_{\beta=1}^{n} h_{k_\beta + \delta^{\beta i}/2}^{\beta}\; f_{\,k+i/2}^{\,m+1}\,, \qquad (10)$$

$$A(\varphi_{k+i/2}^{m+1}) = \int_{V_e^i} \Lambda(\varphi^{\,m+1}) \partial V_e^i + O(h^2) \partial V_e^i\,,$$

$h = \max_j \max_{k_j} h_{k_j}^j$. Operator $A(\varphi_{k+i/2})$ can be written in the following finite difference form:

$$A(\varphi_{k+i/2}) = c_{k+i/2}\,\varphi_{k+i/2} - \\ - \sum_{j=1}^{n}\left(a^{j}_{k+i/2}\varphi_{k-j+i/2} + b^{j}_{k+i/2}\varphi_{k+j+i/2} \right), \tag{11}$$

$$a^{j}_{k+i/2} = \Big(0.5\,\rho_{k-j/2+i/2}\, u^{j}_{k-j/2+i/2} + \\ + (1+\nu^{j}_{k-j/2+i/2})\,\eta^{j}_{k-j/2+1/2} \,/ \\ / h^{j}_{k_j+\delta^{ji}/2-1/2}\Big)\prod_{\beta\neq j}^{n} h^{\beta}_{k_\beta+\delta^{\beta i}/2},$$

$$b^{j}_{k+i/2} = \Big(-0.5\,\rho_{k+j/2+i/2}\, u^{j}_{k+j/2+i/2} + \\ + (1+\nu^{j}_{k+j/2+i/2})\,\eta^{j}_{k+j/2+1/2} \,/ \\ / h^{j}_{k_j+\delta^{ji}/2+1/2}\Big)\prod_{\beta\neq j}^{n} h^{\beta}_{k_\beta+\delta^{\beta i}/2},$$

$$c^{j}_{k+i/2} = \sum_{j=1}^{n}\left(a^{j}_{k+i/2} + b^{j}_{k+i/2} \right),$$

$$\nu^{j}_{k+j/2+i/2} = (\alpha_{k+j/2+i/2}\,\mathrm{cth}\,\alpha_{k+j/2+i/2}) - 1 \tag{12}$$

$$\alpha_{k+j/2k+i/2} = u^{j}_{k+j/2+i/2}\, h^{j}_{k_j+\delta^{ji}/2+1/2} \,/ \\ / 2\eta_{k+j/2k+i/2}.$$

In practical calculations function $(\alpha\,\mathrm{cth}\,\alpha - 1)$ in (12) may be replaced with easily computed expression $\alpha\,\mathrm{cth}\,\alpha - 1 \approx |\alpha|^3 / (1+|\alpha|+|\alpha|^2)$.

3 Linearization Procedure and Implicit Stabilization Method

A pressure discrete equation is obtained using momentum difference equations in the form (10) and difference continuity equation (9). In this case substance φ is a velocity component u^i and right part of (6) contains $-\dfrac{\partial p}{\partial x^i}$. A general form of pressure discrete equation can be presented as

$$\left(\prod_{\beta=1}^{n} h^{\beta}_{k_\beta}\right)\frac{\rho^{m+1}_{k} - \rho^{m}_{k}}{\Delta t_m} + P_h(p_k) = \overline{f_k}, \tag{13}$$

$$P_h(p_k) = \bar{c}_k p_k - \sum_{j=1}^{n} \bar{a}^{j}_{k}\, p_{k-j} + \bar{b}^{j}_{k}\, p_{k+j}.$$

Thus, hydrodynamics discrete problem involves non-linear equations for velocity components, for pressure and in general case state equation.

Implicit stabilization method is developed for solving non-linear system of difference equations. Linearizing is carried out in such a way that operator A becomes linear relatively to $u^{i\,m+1,L+1}_{k+i/2}$, when $u^{i\,m+1,L}_{k+i/2}$ is known, index "L" denotes a number of iteration or a number of stabilization step.

Implicit numerical procedure is written as follows $(1 \le i \le n)$

$$\prod_{\beta=1}^{n} h^{\beta}_{k_\beta+\delta^{\beta i}/2}\,\rho^{m}_{k+i/2}\Bigg(\frac{u^{i\,m+1,L+1}_{k+i/2} - u^{i\,m+1,L}_{k+i/2}}{\tau_L} + \\ + \rho^{m}_{k+i/2}\frac{u^{i\,m+1,L+1}_{k+i/2} - u^{i\,m}_{k+i/2}}{\Delta t_m}\Bigg) + A u^{i\,m+1,L+1}_{k+i/2} = \\ = -\frac{p^{m+1,L+1}_{k+i} - p^{m+1,L+1}_{k}}{h^{i}_{k_i}} + f^{m+1,L}_{k+i/2},$$

$$\prod_{b=1}^{n} h^{\beta}_{k_\beta}\left(\frac{p^{m+1,L+1}_{k} - p^{m+1,L}_{k}}{\tau_L} + \frac{\rho^{m+1,L+1}_{k} - \rho^{m}_{k}}{\Delta t_m}\right) + \\ + P_h\, p^{L+1}_{k} = \overline{f_k},$$

where τ_L is a step of stabilization. It should be noted that linear operator P_h is self-adjoint because $\bar{a}^{j}_{k+j} = \bar{b}^{j}_{k}$.

Successful practical realization of the implicit numerical algorithm depends on a method for solving linear difference equations, first of all ill-conditioned pressure equation. Computational difficulties have been overcame with the usage of incomplete factorization method, first suggested by Buleev [3].

Implicit numerical procedure for prediction of pressure and velocity fields involves the following stages of calculations. Using $u^{i\,m}$, $u^{i\,m+1,L}$ $1 \le i \le n$ from the previous iteration coefficients of difference equations are calculated. Employing incomplete factorization method with Chebyshev acceleration [2] self-adjoint pressure equation is solved and using ordinary variant of the method we calculate velocity components. Iterations on the current time layer are stopped when a preset accuracy ς of fulfilment of difference continuity equation is reached:

$$\max_{\Omega_h}\left|\varsigma_k^{m+1,L+1}\right| < \varsigma \qquad (14)$$

4 Numerical Modeling of Turbulent Two-Phase bubble flow

Developed implicit numerical method in two-dimensional case have been realized as **FLUID2D** code. The code has found various applications and one of them is numerical prediction for turbulent two-phase flow with "saddle"-shape void fraction profile. The recent experimental investigations (e. g. [4–6]) in a local characteristics complex study of bubble non-equilibrium two-phase flows have revealed, in particular, the effects of anomalous wall friction factors and heat transfer coefficients increase in the conditions with predominantly wall concentration (void peak) of gas (vapor) phase at low velocities of forced flow. Due to non-uniform distribution of gas over the tube cross section in upward gas-liquid flows, wall shear stresses can be by 2÷9 times higher than for single-phase flow.

Mathematical and numerical modeling of above mentioned regimes of gas-liquid flows is complicated problem, so one purpose of numerical investigations is to obtain velocity, pressure fields and shear stresses using experimental radial void fraction profiles. Two-phase flow density is calculated as $\rho=(1-\alpha)\rho_f+\alpha\rho_g$, where α - void fraction, ρ_f and ρ_g – density of fluid and gas correspondingly. Hydrodynamics equations are written in the *(r-z)* –geometry for the round pipe of radius *R*.

Turbulent viscosity μ_t is subdivided into the two components $\mu_t=\mu_1+\mu_2$, one μ_1 due to inherent liquid turbulence independent of relative motion of bubbles and the other μ_2 due to the additional turbulence caused by bubble agitation. More detailed mathematical model is described in [7-8].

It should be noticed that boundary layers are very thin therefore correct shear stress description demands detailed grid near wall. Implicit numerical method allows to employ high irregular grid with logarithmic compressibility in the boundary layers zones. Some results of numerical studies for two-phase upward bubble flow are presented in fig. 1-3. The velocity profile, the radial void fraction distribution in the outlet cross-section of the pipe (diameter 86.3 mm) are shown in Fig. 1. Entrance fluid velocity is $U_f = 0.79$ m/s, volumetric void fraction β=0.118.

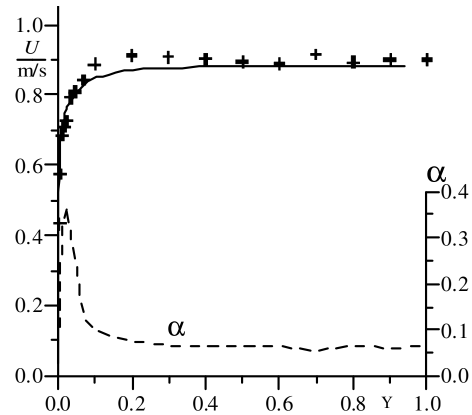

Fig. 1: Liquid axial velocity and void fraction profile; — - calculation, ✚ - experimental data; - - - –void fraction.

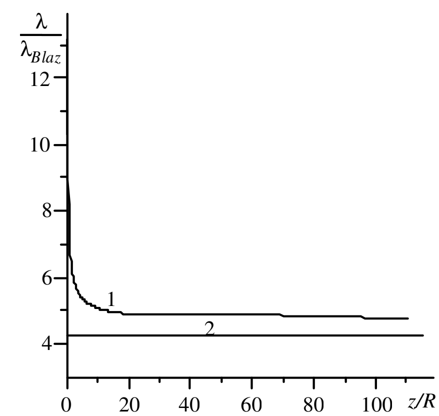

Fig. 2: Relative friction factor; 1 – calculation, 2- experiment.

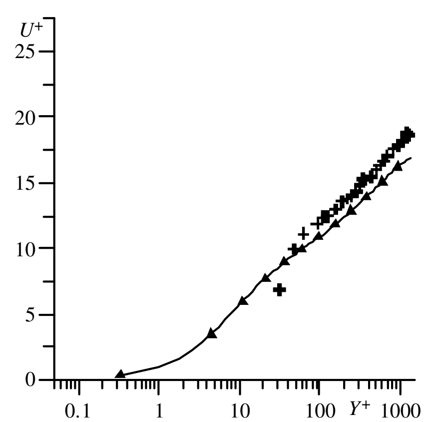

Fig. 3. Liquid axial velocity, *R*=21 mm, β=0.02, $U_f = 0.82$ m/s; ▲ - calculation, ✚ - experiment.

Proceedings of the 4th WSEAS International Conference on Fluid Mechanics and Aerodynamics, Elounda, Greece, August 21-23, 2006 (pp136-141)

Relative friction factor presented in fig 2 shows essential increase in comparison with Blasius factor for single–phase flow. Numerical results are in the satisfactory agreement with experimental data [4].

In fig. 3 velocity profiles are presented in dimensionless form, where $Y = 1 - r/R$,

$Y^+ = \rho Y u_\tau / \mu_m$ – dimensionless coordinate,

$u_\tau = \sqrt{\tau_w / \rho}$ - friction velocity; τ_w – wall shear stress; $u^+ = u_z / u_\tau$ - friction scale velocity.

It can be seen that numerical model describes boundary layer zone with good accuracy up to $Y^+ < 1$.

5 Numerical Results for 3-D Convection Benchmark Problem

Three-dimensional case of implicit numerical method is realized as **FLUID3D** code. As a test of the numerical method and the code benchmark computations have been performed. The papers [9, 10] contains experimental results for heat convection in a cubical air-filled enclosure. This problem is suggested as 3-D benchmark exercise. A sketch of the experiments [9, 10] is shown in Fig. 4.

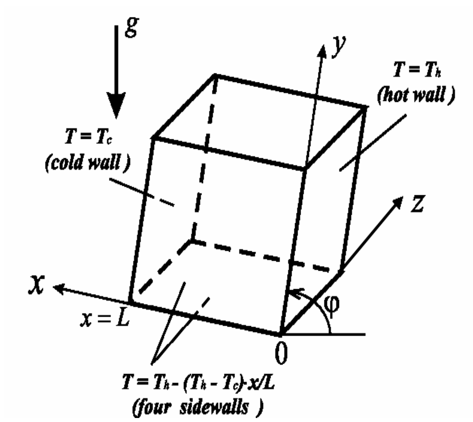

Fig. 4. Schematics of the cubical cavity benchmark.

Width of the cubic is L=0.1272m, the inclination angle φ is set to 0°, 45°, and 90°, the cube sidewall temperature varies linearly from cold face to hot face, $T_c = 300\,\mathrm{K}$, $T_h = 307\,\mathrm{K}$. Gas properties are evaluated at the mean temperature $T_m = 303.5\,\mathrm{K}$, Pr=0.71, the pressure is equal to the pressure that gives the desired Rayleigh number.

Calculations are conducted using uniform and non-uniform grids and different number of grid nodes: 40^3, 60^3, 100^3. Some numerical results and comparisons are presented in the table 1 and fig. 5-8.

Table 1. Average Nusselt Number results

φ	Ra	Exp. Nu [9, 10]	Present paper	[11]	[12]
90	10^6	6.383 ± 0.070	6.51	7.20-7.33	6.43
90	10^7	12.98 ± 0.16	13.13	16.62-16.94	13.10
90	10^8	26.79 ± 0.34	26.54	37.92-38.39	24.99
45	10^6	8.837 ± 0.101	9.04	8.52-8.63	8.61
45	10^8	34.52 ± 0.42	32.02	44.67-44.83	28.35
0	10^6	7.883 ± 0.091	7.77-7.96	7.31-7.42	7.57

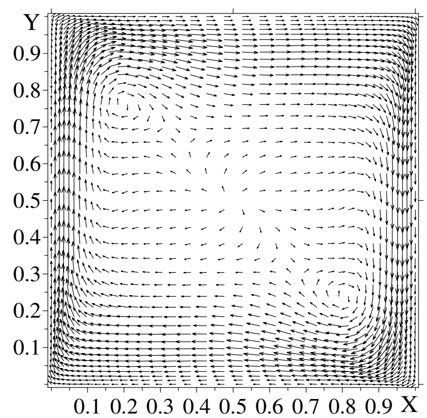

Fig. 5. Flow patterns in the plane z=0.5, $\varphi = 90°, Ra = 10^6$.

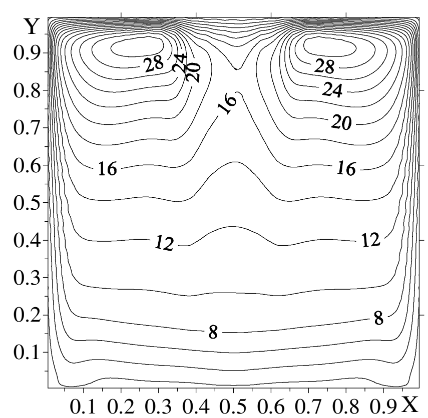

Fig. 6. Distribution of the local Nusselt number on the cold wall, $\varphi = 90°, Ra = 10^7$.

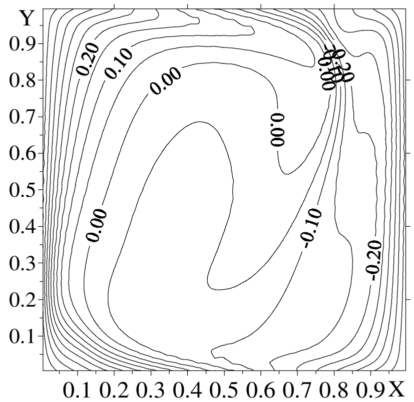

Fig. 7. Temperature contours in the plane z=0.5, $\varphi = 45°, Ra = 10^6$.

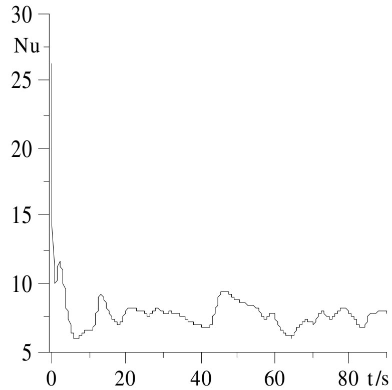

Fig. 8. Average Nusselt number on the cold wall, $\varphi = 0°, Ra = 10^6$

6 Conclusion

Implicit numerical method for solving 2D and 3D-dimensional fluid mechanics, heat and mass transfer equations is described. Implicit method is stable and convergent, enables to enlarge time step and reduce computational expenditures. Presented results of 2D two-phase flow and 3D natural convection numerical studies show potential possibilities of the method. Good agreement with experimental data is reached.

Acknowledgments. This work was supported by the Russian Foundation for Fundamental Studies and Government of Kaluga Region under Grant № 04-01-97216.

References:

[1] Artemyev V.K., Implicit Method for Solving of Navier-Stokes Equations in Natural Variables, *Modeling in Mechanics*, Novosibirsk, Vol. 6(23), N 1, 1992, pp. 17–22.

[2] Artemyev, V.K., *Development of Numerical Methods for Solving Fluid Dynamics Problems*, Thesis, Institute of Physics and Power Engineering, Obninsk, Russia, 1997.

[3] Buleev N.I., A Numerical Method for Solution of Two-Dimensional and Three-Dimensional Equations of Diffusion, *Mat. Sb.*, 51, N 2, 1960, pp. 227–238.

[4] Nakoryakov V.E., Kashinsky O.N., Local Characteristics of Upward Gas-Liquid Flows, *Int. J. Multiphase Flow*, Vol. **7,** 1981, pp. 63–81.

[5] Kashinsky, O.N., & Randin, V.V., Downward Bubbly Gas-Liquid Flow in a Vertical Pipe, *Int. J. Multiphase Flow*, Vol. 25, 1999, pp. 109-138.

[6] Sato Y., Sadatomi M., Sekoguchi K., Momentum and Heat Transfer in Two-Phase Bublbe Flow-II A Comparison between Experimental Data and Theoretical Calculations, *Int. J. Multiphase Flow*, Vol. 7, 1981, pp. 179–190.

[7] Artemyev V.K., Kornienko Yu.N. Two-Dimensional Modeling of Two—Phase Bubble Flows on the Basis of Single-Fluid Description. Method and Algorithm, *Communications of Higher Schools. Nuclear Power Engineering,* N 1, 2003, pp. 88–96.

[8] Artemyev V.K., Kornienko Yu.N. Numerical Studies of Non-Monotone Void Fraction Profiles Effects on Hydrodynamics and Heat Transfer in Two-Phase Bubble Flows. Comparison with Experiment, *Communications of Higher Schools. Nuclear Power Engineering,* N 2, 2003, pp. 78–87.

[9] Leong W.H., Hollands K.G.T., and Brunger A.P., On a Physically-realizable Benchmark Problem in the Internal Natural Convection, *Int. J. Heat Mass Transfer*, 1998, Vol. 41, pp. 3817–3828.

[10] Leong W.H., Hollands K.G.T., and Brunger A.P., Experimental Nusselt numbers for a cubical-cavity benchmark problem in natural convection, *Int. J. Heat Mass Transfer*, 1999, Vol. 42, pp. 1979–1989.

[11] Mossad R., Prediction of Natural Convection in an Air-Filled Cubical Cavity using Fluent Software, *ICHMT 2nd Int. Symp. on Adv. in Comput. Heat Transfer*, Palm Cove, Queensland, Australia, May 20-25, 2001, pp. 1371–1376.

[12] Krepper K., CHT'01: Validation Exercise: Natural Convection in an Air-Filled Cubical Cavity, *ICHMT 2nd Int. Symp. on Adv. in Comput. Heat Transfer*, Palm Cove, Queensland, Australia, May 20-25, 2001, pp. 1351–1356.